Rotational Dynamics of Fullerenes in the Molecular Crystal of Fullerite

Mikhail Alekseevich Bubenchikov, Alexey Mikhailovich Bubenchikov, Aleksandr Viktorovich Lun-Fu, and Vyacheslav Aleksandrovich Ovchinnikov*

The work is devoted to the study of gyroscopic phenomena in the interaction of a rotating fullerene molecule and a xenon atom incident on it. The methods of classical molecular physics are used: intermolecular potentials, Newton's equations for describing the motion of particles, and the Runge–Kutta numerical method of high order of accuracy. A mathematical model is constructed and implemented for the rotation frequencies of fullerene up to 10^{14} Hz and the speed of the incident xenon atom of the order of 10^3 m s^{-1}. For such parameters of the problem, the de Broglie wavelength of the incident atom and the fullerene molecule become smaller than the diameter of the carbon atomic nucleus. This made it possible to apply the Newtonian approach without involving quantum mechanics. The aim of this work is the consistent application of the apparatus of classical mechanics to reveal the effect of the precession of rotating fullerene inside fullerite.

1. Introduction

Fullerene-based materials possess a wide range of unique physical and chemical properties such as high hardness at low density, low or high thermal conductivity depending on conditions, high thermal stability, fire resistance, and so on.[1] A whole group of both theoretical and experimental works is directly focused on revealing the effect of increasing the hardness of fullerene-containing materials.[2–12]

Under normal conditions, C_{60} molecules are located at the sites of the crystal lattice of the fullerite crystal and interact with each other through the weak van der Waals forces. Under these conditions, they have a relatively low hardness.[2,3] To increase the hardness, fullerites are polymerized under the influence of elevated temperature and pressure.[4] However, all polymerized fullerite structures have lower values of the bulk modulus of elasticity than that of diamond.[5–8] It is concluded that the crystalline phases of C_{60} have mechanical characteristics that are 2–3 times lower than those of diamond.[9]

Also of great interest is a method for creating fullerene-containing materials with new properties, based on the interaction of accelerated ions with fullerite films. It has been shown that the implantation of ions leads to destruction and strong fragmentation of a C_{60} molecules or knocking out a carbon atom from the C_{60} skeleton.[13–16] As is known, fullerene molecules in a fullerite crystal perform rotational motions with average angular velocities of the order of 10^{11} rad s^{-1}.[17,18] It is also noted that fullerene molecules can be set in rotational motion due to the action of laser pulses.[19] The interaction of elastic and plastic deformations of the fullerite lattice with the effects of orientational ordering, rotation, and librational vibrations of molecules is highlighted.[20] It was shown that, due to thermal excitation of the rotational degrees of freedom, the chaotic rotation of C_{60} molecules increases, ensuring energy efficiency and stability of the close-packed face-centered cubic (fcc) structure.[21] The features of rotating molecules can be used to reduce external force to redistribute the load on a group of atoms belonging to fullerene. This will prevent the knockout of an individual atom or an entire fragment from the C_{60} skeleton.

Of particular interest is the study of the precessional motion of the nodes of a molecular crystal, within the framework of which a gyroscopic effect can arise, which is important from the point of view of changing the characteristics of a material. In most modern works on this topic, the term "gyroscope" is used rather in the sense of a molecular rotor.[22] Only a few researchers actively tried to design working devices based on it.[23–25] Even fewer of them concerned the direct consideration of gyroscopic phenomena inside crystal structures. Using the gyroscopic effect, it is possible to stabilize the fullerene molecule near its equilibrium position and increase the internal resistance to external influences on the material surface.

It was shown that C_{60} performs various types of nanomotions with rotation and switching between different orientations.[26] To create the best gyroscopic effect, it is necessary to select

Prof. M. A. Bubenchikov, Dr. A. M. Bubenchikov
Department of Theoretical Mechanics
National Research Tomsk State University
36 Lenin Ave., Tomsk 634050, Russia

A. V. Lun-Fu
LLC "Gazprom Transgaz Tomsk"
9 Frunze St., Tomsk 634029, Russia

Dr. V. A. Ovchinnikov
Department of Physical and Computational Mechanics
National Research Tomsk State University
36 Lenin Ave., Tomsk 634050, Russia
E-mail: empiric@mail.ru

the correct direction of rotation. A fullerene molecule filled with a magnetic material can be oriented using an external magnetic field.[27] The temperature dependences of the magnetic properties of fullerite C_{60} were also investigated.[28] It should be noted that changes in the initial characteristics of fullerite significantly affect the properties of synthesized carbon particles.[10]

The quantum mechanical approach can be used to study gyroscopic effects.[29] However, this approach has much more grounds for application in the region of low temperatures, which determine the state of the material. P. M. Rafailov et al. investigated the rotational dynamics of fullerites by measuring Raman-active intramolecular modes at different temperatures.[30] A. Piatek et al. simulated the dynamics of C_{60} fullerenes by the molecular dynamics method in a cluster consisting of seven C_{60} molecules.[31] The interaction is taken as the full 60-site Lennard–Jones (LJ) pairwise additive potential, which generates the translational and rotational motions of each molecule.

In the current article, we simulate the dynamic state of a microcanonical ensemble of 13 fullerenes using a classical molecular dynamics. The estimated calculations predict an increase in the hardness of fullerite due to the creation of oriented rotations of magnetically susceptible fullerenes in external magnetic fields.

2. Statement of the Physical Problem

In this article, we simulate the dynamic properties of the rotating C_{60} molecule surrounded by 12 C_{60} molecules when interacting with an incident particle (**Figure 1**). The rotational motion of the fullerene is described using the Euler approach. The interaction of the particle with the central fullerene carbon atoms is described on the basis of the LJ potential. The particle moves in the direction of the central C_{60} molecule at an initial velocity of $600\,\mathrm{m\,s^{-1}}$ (see Figure 1). The xenon atom (Xe, 131 a.m.) was used as the particle. The initial angular velocity ω^0 of the C_{60} molecule ranged from 0 to $10^4\,\mathrm{rad\,ns^{-1}}$.
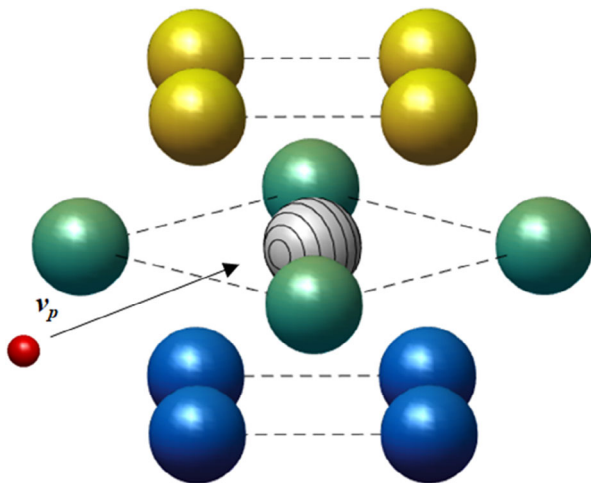

Figure 1. Scheme of interaction between a particle and a rotating fullerene surrounded by other fullerenes. Red color corresponds to the xenon atom.

3. Statement of the Mathematical Problem

We introduce some absolute (fixed) Cartesian coordinate system $0xyz$, at the beginning of which we place the center of the rotating fullerene C_{60}, as well as the Cartesian coordinate system $C\xi\eta\zeta$, associated with the moving fullerene and its center of mass C. Let the particle be at a certain distance from the C_{60} molecule, on which the forces of the van der Waals interaction are small, and moves with velocity v_p in the direction of fullerene (see Figure 1). Rotating and moving fullerene will be considered as a skeleton structure consisting of carbon atoms. The interaction of a specific carbon atom with a particle will be determined using a potential that defines two classes of forces: repulsion and attraction. The LJ potential is suitable for this purpose.

$$U(r_{pk}) = 4\varepsilon \left[\left(\frac{\sigma}{r_{pk}} \right)^{12} - \left(\frac{\sigma}{r_{pk}} \right)^{6} \right] \tag{1}$$

where r_{pk} is the distance between the incident atomic particle and the kth fullerene atom.

The rotating C_{60} molecule is located in a node of a fcc lattice. Its immediate surroundings are 12 C_{60} molecules. The surrounding fullerenes have a smoothed spherical potential.[32] Initially, their centers are located at a distance of 1.002 nm from the origin of the $0xyz$ coordinate system.

$$\Phi(r_{ik}) = \frac{4\varepsilon\pi a}{r_{ik} S_1} \left[\frac{\sigma^{12}}{5} \left(\frac{1}{(r_{ik} - a)^{10}} - \frac{1}{(r_{ik} + a)^{10}} \right) - \frac{\sigma^6}{2} \left(\frac{1}{(r_{ik} - a)^4} - \frac{1}{(r_{ik} + a)^4} \right) \right] \tag{2}$$

Here S_1 is the area per carbon atom; a is the radius of fullerene; r_{ik} is the distance between the center of the ith adjacent fullerene and the kth carbon atom of the considered C_{60} molecule, $i = 1,\ 12,\ k = 1,\ 60$. Function (2) determines the interaction energy between a fullerene and an individual xenon or carbon atom. This function determines the van der Waals effect from an infinitely thin homogeneous spherical layer. It also determines the infinite repulsion when the moving particle approaches the specified layer.

In contrast to L. A. Girifalco's articles, our description contains two models of fullerenes: a central fullerene with icosahedral symmetry and the spherical fullerenes surrounding it.[33,34] Icosahedral fullerene has all the properties of a real fullerene. Spherical fullerenes affect it as idealized spheres.

3.1. Angular Vibrations and Rotations of Fullerenes

To describe the rotational motion of a fullerene molecule around its own center of mass, the projections of the angular momentum equation on the ξ, η, and ζ axes are used

$$A\frac{dp}{dt} + (C - B)qr = M_\xi^{(e)} \tag{3}$$

$$B\frac{dq}{dt} + (A - C)rp = M_\eta^{(e)} \tag{4}$$

$$C\frac{\mathrm{d}r}{\mathrm{d}t} + (B - A)pq = M_{\zeta}^{(e)} \tag{5}$$

Here p, q, r are the projections of the angular velocity on the ξ, η, and ζ axes; A, B, C are the main moments of inertia of the molecule for its center of mass.

The projections of the moments of forces in formulas (3)–(5) on the axes of the $C\xi\eta\zeta$ coordinate system connected with the central fullerene are determined by the following equations.

$$M_{\xi}^{(e)} = a_{11}M_x^{(e)} + a_{12}M_y^{(e)} + a_{13}M_z^{(e)} \tag{6}$$

$$M_{\eta}^{(e)} = a_{21}M_x^{(e)} + a_{22}M_y^{(e)} + a_{23}M_z^{(e)} \tag{7}$$

$$M_{\zeta}^{(e)} = a_{31}M_x^{(e)} + a_{32}M_y^{(e)} + a_{33}M_z^{(e)} \tag{8}$$

where $\{a_{ij}\}$ $(i, j = \overline{1, 3})$ is the matrix of direction cosines connecting the coordinate systems $0xyz$ and $C\xi\eta\zeta$. The components of this matrix are trigonometric functions of Euler angles: proper rotation—φ, precession—ψ, and nutation—θ. The matrix is called the rotation matrix.

The projections of the moment of forces external $M_x^{(e)}$, $M_y^{(e)}$, $M_z^{(e)}$ to the fullerene under consideration on the axis of the absolute basis are determined from the following formulas.

$$\mathbf{M}^{(e)} = \sum_{k=1}^{S}\sum_{i=1}^{N+1} \mathbf{M}_{ik}^{(e)}; \quad \mathbf{M}_{ik}^{(e)} = [\mathbf{r}_{kc}, \mathbf{F}_{ik}] = \begin{vmatrix} \mathbf{i} & \mathbf{j} & \mathbf{k} \\ x_{kc} & y_{kc} & z_{kc} \\ X_{ik} & Y_{ik} & Z_{ik} \end{vmatrix} \tag{9}$$

Here $\mathbf{M}_{ik}^{(e)}$ is the moment of force $\mathbf{F}_{ik}$ taken relative to the center of mass of the molecule; $\mathbf{r}_{kc}$ is the radius vector of the atom relative to the center of mass of the molecule; $\mathbf{i}, \mathbf{j}, \mathbf{k}$ are the unit vectors of the $0xyz$ coordinate system; the value $i = N + 1$ corresponds to a moving particle.

The force effect on each atom of a rotating C_{60} molecule can be determined by the following formulas.

$$X_{ik} = -\frac{\partial U}{\partial x}(r_{ik}), \quad Y_{ik} = -\frac{\partial U}{\partial y}(r_{ik}), \quad Z_{ik} = -\frac{\partial U}{\partial z}(r_{ik}) \tag{10}$$

Here, X_{ik}, Y_{ik}, Z_{ik} are the projections of the forces on the axes of the $0xyz$ coordinate system acting on the kth atom of the C_{60} rotating molecule from the ith surrounding fullerene or the atomic particle.

Equation (3)–(5) are closed by Euler's kinematic relations, which are usually written in a form that is not resolved with respect to the time derivatives of the Euler angles.

$$p = \dot{\psi}\sin\theta\sin\varphi + \dot{\theta}\cos\varphi \tag{11}$$

$$q = \dot{\psi}\sin\theta\cos\varphi - \dot{\theta}\sin\varphi \tag{12}$$

$$r = \dot{\psi}\cos\theta + \dot{\varphi} \tag{13}$$

Here, a dot is placed above the function name to denote the time derivative of a function.

3.2. Movement of the Centers of Mass of Fullerenes and Particle

To determine the motion of the centers of mass of fullerenes, the equations are given below.

$$M\frac{\mathrm{d}\mathbf{v}_c}{\mathrm{d}t} = \sum_{k=1}^{S} \nabla U(r_{pk}) + \sum_{k=1}^{S}\sum_{i=1}^{N} \nabla\Phi(r_{ik}), \quad \mathbf{v}_c = \frac{\mathrm{d}\mathbf{r}_c}{\mathrm{d}t} \tag{14}$$

The translational motion of an atomic particle is governed by the law of change in the momentum of this particle.

$$m_p\frac{\mathrm{d}\mathbf{v}_p}{\mathrm{d}t} = \sum_{i=1}^{N} \nabla\Phi(r_{pi}) + \sum_{k=1}^{S} \nabla U(r_{pk}), \quad \mathbf{v}_p = \frac{\mathrm{d}\mathbf{r}_p}{\mathrm{d}t} \tag{15}$$

Here M is the fullerene mass, m_p is the particle mass, ∇ is the gradient operator; $S = 60$ is the number of carbon atoms in the C_{60} molecule; $N = 12$—the number of surrounding fullerenes; r_{pk} is the distance from the center of the particle to the center of the kth carbon atom on the moving fullerene; r_{pi} is the distance from the center of the particle to the center of the ith surrounding fullerene; r_{ik} is the distance between the kth atom of the considered fullerene and the center of the ith fullerene from the group of the remaining 12 C_{60} molecules. Index "c" defines the center of the rotating fullerene, "p" refers to the particle. The potential U is determined by formula (1), Φ is by formula (2).

3.3. Initial Conditions and Integration Scheme

The initial conditions for solving the system of differential Equation (3)–(5) and (11)–(13) are given in the following form.

$$t = 0: \psi = \psi^0, \theta = \theta^0, \varphi = \varphi^0; p = p^0, q = q^0, r = r^0$$
$$\mathbf{v}_c = \mathbf{v}_c^0, \mathbf{r}_c = \mathbf{r}_c^0, \mathbf{v}_p = \mathbf{v}_p^0, \mathbf{r}_p = \mathbf{r}_p^0 \tag{16}$$

The initial values of the Euler angles $\psi^0, \theta^0, \varphi^0$ for all fullerenes can be assumed to be zero without loss of generality. The initial rotational velocities of fullerenes p^0, q^0, r^0 should be such that the angular velocity $\omega^0 = \sqrt{(p^0)^2 + (q^0)^2 + (r^0)^2}$ corresponds to a given rotational temperature. The initial velocity $\mathbf{v}_c^0$ must correspond to the given vibrational temperature. Taken together, the initial coordinates $\mathbf{r}_c^0$ should determine the arrangement of fullerenes in the fcc lattice. The velocity $\mathbf{v}_p^0$ of the atomic particle and the initial position $\mathbf{r}_p^0$ should ensure its passage through the barrier of the fullerene surroundings and collision with the central fullerene.

The numerical solution of problem (3)–(5), (11)–(13), (16) is carried out using the Runge–Kutta scheme of the fourth order of accuracy,[35] which allows determining the trajectories of particles and the center of mass of a moving fullerene molecule, as well as rotation angles of the fullerene under consideration. Software for modeling the impact of an incident particle on the dynamics of a rotating fullerene molecule in a fullerite crystal was created using the Fortran programming language and the GNU Fortran compiler.

4. Results of Numerical Calculations

Calculations of the dynamics of a rotating C_{60} fullerene molecule interacting with an incident Xe particle and surrounding lattice sites were carried out for the following parameters: the radius of the spherical C_{60} $a = 0.354$ nm; the energy of the carbon–carbon interaction; and the radius of the zero energy value $\varepsilon_1/k = 51.2$ K, $\sigma_1 = 0.3653$ nm, the Xe–Xe interaction energy and the corresponding radius $\varepsilon_2/k = 229$ K, $\sigma_2 = 0.4055$ nm, where $k = 1.38 \times 10^{-23}$ J K^{-1} is the Boltzmann constant. Interaction of different pairs of atoms was determined using average values of energy and radius: $\sigma = (\sigma_i + \sigma_j)/2$, $\varepsilon = \sqrt{\varepsilon_i \varepsilon_j}$. Since formula (2) is obtained from the LJ potential (1), ε and σ in (2) are already average values corresponding to interactions of dissimilar pairs (C_{60}–Xe) or identical pairs (C_{60}–C).

4.1. Interaction of a Single Fullerene with an Incident Particle

We consider the interaction of a particle moving with an initial velocity $\mathbf{v}_{px}^0 = 600$ m s^{-1} toward a single C_{60} molecule rotating with an initial angular velocity $\omega^0 = 10^4$ rad ns^{-1}. Let the axis of rotation be oriented in the direction of the x-axis, i.e., the components of the angular velocity (p, q, r) are as follows $(\omega^0, 0, 0)$. We take a xenon atom (Xe, 131 amu) as an incident particle. It is convenient to take the ζ-axis as the axis of rotation for the initial moment of time. The angles ψ, θ will determine the further orientation of this axis in space.

Figure 2 shows the trajectory of the movement of molecules and xenon in the $0xy$ plane. At the initial time, Xe is at the point $(-4, 0.4, 0)$, C_{60} is $(0, 0, 0)$. The figure shows that the Xe particle, approaching the fullerene, deviates from its initial direction of motion and continues to move at an angle to the x-axis. The fullerene molecule also moves from its initial position. It is worth noting that, according to the calculations, the motion of the C_{60} molecule and the Xe particle is three-dimensional, since the forces acting on them are crossed forces, i.e., they do not lie in the same plane.

The region of maximum intermolecular interaction of a particle and a C_{60} molecule is of interest. We study the effect of the
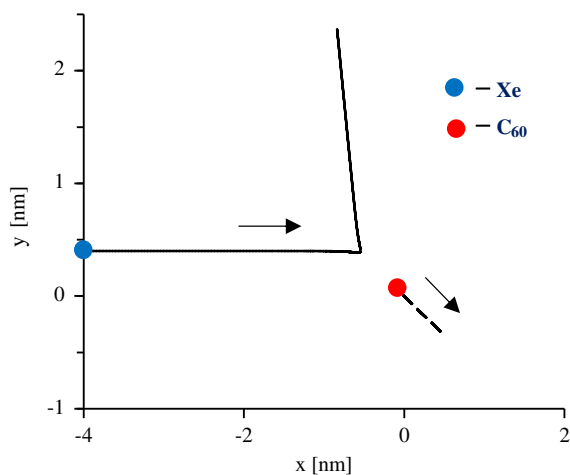

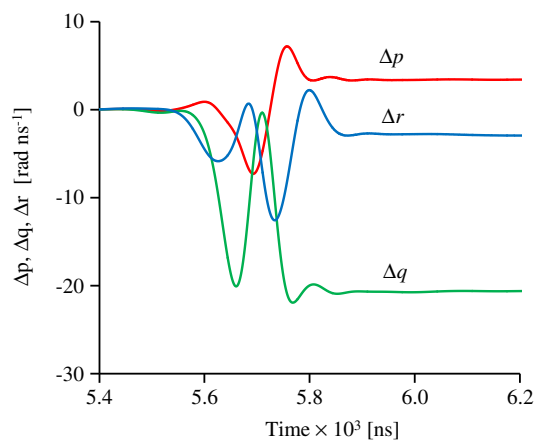**Figure 2.** The trajectory of Xe and C_{60} in the absence of surrounding fullerenes.

Figure 3. Time dependences of Δp, Δq, Δr at $\omega^0 = 10^4$ rad ns^{-1}.

"impact" of a particle on the precession motion of the rotating fullerene C_{60} at times where this interaction is greatest. **Figure 3** shows the time dependences of the quantities

$$\Delta p = p - p_0, \quad \Delta q = q - q_0, \quad \Delta r = r - r_0 \quad (17)$$

which characterize the change in the projections of the angular velocity of the fullerene C_{60} relative to their values at the initial moment of time.

The figures show that when the particle approaches the fullerene molecule, vibrational changes in the orientation of the axis of rotation are observed. A change in the components of the angular velocity (p, q, r) during the interaction of the incident particle with rotating fullerene indicates the presence of precessional movements of the C_{60} fullerene. After the particle is at a sufficiently large distance from the fullerene C_{60}, the components of the angular velocity are set at constant values.

4.2. The Interaction of Fullerene with the Surroundings

Here, we study the interaction of a rotating C_{60} molecule with the surrounding fullerenes depending on the initial rotation speed $\omega^0 = 0$, 1000, 1100 rad ns^{-1}. The rotating C_{60} molecule is located in the center of the isolated microcanonical volume and is surrounded by 12 C_{60} molecules. Let the rotation axis be oriented in the direction of the x-axis, i.e., components of the angular velocity $(p, q, r) = (\omega^0, 0, 0)$.

Figure 4 shows the dependences of the angle θ on time at $\omega^0 = 0$, 1000, 1100 rad ns^{-1} (curves 1, 2, 3, respectively). In the case under consideration, the change in the angles φ and ψ is negligible compared to the angle θ. This suggests that angular movements occur around the x-axis. Figure 4 shows that fullerene undergoes nutational fluctuations around the axis $\theta = \pi/2$ at $\omega^0 = 0$ and 1000 rad ns^{-1}. The behavior of curve 3 indicates that fullerene rotates around the x-axis with weakly expressed nutational fluctuations at $\omega^0 = 1100$ rad ns^{-1}.

Figure 5 illustrates the change in angular velocity with time at $\omega^0 = 0$, 1000, 1100 rad ns^{-1} (curves 1, 2, 3, respectively). At $\omega^0 = 0$, 1000 rad ns^{-1}, the fullerene molecule undergoes periodic angular oscillations with a change in the angular velocity ω from
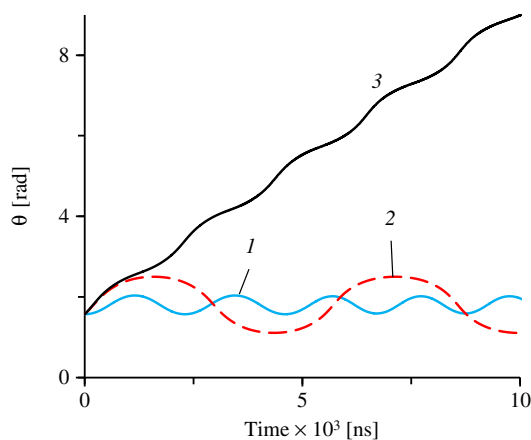
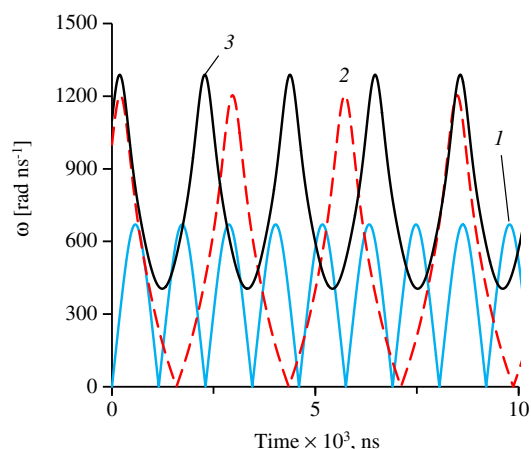**Figure 4.** The dependence of the angle θ on time.

Figure 5. The dependence of the angular velocity on time.

0 to 670 rad ns^{-1} (curve 1) and 0 to 1204 rad ns^{-1} (curve 2). Reaching zero values of ω means that the direction of the angular velocity vector of fullerene changes. At the initial angular velocity $\omega^0 = 1100$ rad ns^{-1}, a steady rotational motion is observed with a

change in the angular velocity from 405 to 1288 rad ns^{-1}. The change in the magnitude of the angular velocity (see Figure 5, curves 1–3) is due to the force action of 12 surrounding fullerenes, which at some points in time counteract the rotational motion of the C_{60} molecule, and at others they increase this rotation.

The performed calculations demonstrate that throughout the considered time, the rotating fullerene will stably maintain its position at different ω^0. Note that this happens when the center of the rotating fullerene at the initial moment of time is at the point (0, 0, 0). This result allows in the future to carry out a numerical experiment to assess the influence of the incident particle on the position of the rotating fullerene.

4.3. The Effect of an Incident Particle on a Rotating Fullerene with Its Surroundings

We consider a system consisting of an incident Xe particle, a central C_{60} molecule, and 12 surrounding fullerenes depending on the initial angular rotation velocity $\omega^0 = 0$, 1000, 1100 rad ns^{-1}. At the initial moment of time, the incoming particle is in the position (–4, 0, 0) and has a velocity $v_{px}^0 = 600$ m s^{-1}. We impart a rotational motion to the fullerene along the x-, y-, z-axes.

The trajectories of one of the atoms of the rotating fullerene are shown in **Figure 6** for these three options. In the case when the angular velocity at the initial moment of time equals (ω^0, 0, 0), the selected atom first moves along a circular path (dashed curve) relative to the x-axis (Figure 6a). After interacting with the incident particle (solid curve), the central fullerene, in addition to the rotational motion, begins to additionally perform nutational displacements due to the translational motion of the fullerene center of mass along the x-axis. They persist even after the incident particle is removed at a considerable distance. At initial angular velocities $\omega = (0, \omega^0, 0)$ and $(0, 0, \omega^0)$ corresponding to Figure 6b,c, the instantaneous axis of rotation changes direction (dashed curve). This suggests that in these cases, the precession motion is observed before interacting with the incident particle. As a result of interaction with the incident
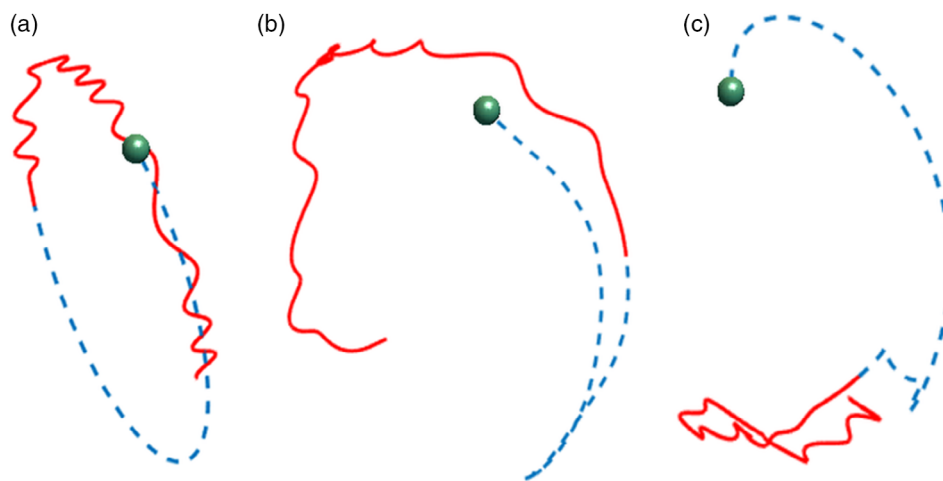

Figure 6. The trajectory of the atom of a rotating fullerene obtained at a) $\omega^0 = (\omega^0, 0, 0)$, b) $\omega^0 = (0, \omega^0, 0)$, and c) $\omega^0 = (0, 0, \omega^0)$.
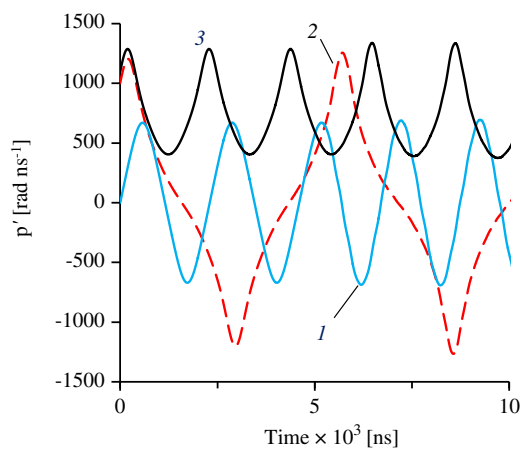
Figure 7. The projection of the angular velocity on the *x*-axis.

particle, the nutation movement is superimposed on the precession motion.

Figure 7 shows the time dependences of the projection of the angular velocity p' on the *x*-axis. Curves 1, 2, 3 in Figure 7 correspond to angular velocities $\omega^0 = 0, 1000, 1100$ rad ns^{-1}, respectively. Considering the effect of the incident particle leads to a small increase in the amplitude and period of changes in the angular velocity for $\omega^0 > 0$. Moreover, the behavior of the curves shown in Figure 7, qualitatively similar to the case without an incident particle.

Figure 8 shows the temporal changes in the coordinates (x_c) of the center of the rotating fullerene at $\omega^0 = 0, 1000, 1100$ rad ns^{-1} (curves 1, 2, 3, respectively). The circles show the local extrema of the displacement of the fullerene center at $\omega^0 = 0$ rad ns^{-1}. Coordinates y_c, z_c in the considered time interval have much smaller changes, therefore, they are not presented here. As can be seen from Figure 8, the fullerene center shifts relative to the initial position after exposure to the incident particle. For the considered time period from 0 to 0.1 ns, the difference in the mean deviations for $\omega^0 = 1000$ and 1100 rad ns^{-1} was about 0.1%. The average deviation was determined as the sum of the local extrema of the function $x_c(t)$ (circles in Figure 8)
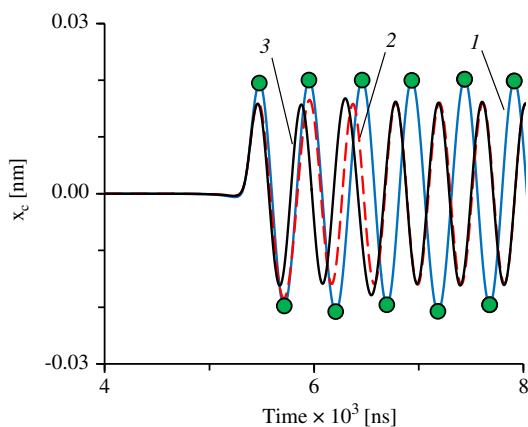

Figure 8. Temporary change in the x_c coordinate of the center of a rotating C_{60} molecule.

related to their number. The average deviation at $\omega^0 = 0$ rad ns^{-1} is 0.0201 nm, at $\omega^0 = 1000$ rad ns^{-1} is 0.0163 nm. Therefore, a large initial angular velocity leads to a decrease in the displacement of the fullerene molecule by 18.8%.

5. Conclusion

The results of the calculations showed that when a particle interacts with a rotating fullerene, there is a precessional motion. Surrounding fullerenes strongly affect the change in the angular velocity of a rotating molecule. It was found that the displacement of the fullerene relative to its initial position depends on the choice of the initial angular velocity.

For the highest of the considered angular velocities, it was possible to reduce the displacement of the C_{60} fullerene by 18.8% in comparison with the case $\omega^0 = 0$ rad ns^{-1}. This suggests that the rotating fullerene due to the strength of the gyroscopic reaction is able to balance the external effect. This feature of the rotating C_{60} molecule can be used to enhance the ability of fullerene-containing materials to counteract dynamic indentation deformation.

6. Discussion

Since the purpose of this article is to study the gyroscopic properties of untwisted fullerene located in the minimal fullerene surroundings of the molecular crystal. This local goal was achieved without considering fluctuations of carbon atoms in the molecules of fullerenes. Although within the framework of the considered approach, it is not difficult to take into account these fluctuations.[36] Another argument in favor of the simplifications used in this article is that the group of rotations of fullerenes and the group of their translational displacements are independent. At least in the sense that completely independent equations are used for them. For the angular momentum, this is the vector equation of moments; for the vibrations of molecules, these are the vector equations of motion of their centers of mass. This approach allows the use of a sufficiently large number of crystal nodes with periodicity conditions at the boundaries of the selected material fragment.

In this case, the energy of such a system of nodes is conserved or changed due to heat exchange at the boundaries of the fragment. Based on the results of calculations of such a system, all average statistical characteristics are determined, such as vibrational temperature, rotational temperature, etc.

Moving on the way of further simplification of the mathematical model, we considered an isolated system consisting of a single untwisted node and twelve nodes that make up its closest surroundings in the crystal, as well as a single atom moving in tunnels between nodes. Thus, a microcanonical ensemble was isolated, in which a relatively free xenon atom affected the central fullerene of the selected ensemble and caused its precession motion. At the same time, the energy of the system was conserved. In this setting, all collisions were elastic. To analyze the energy dissipation of a moving atom, a too small piece of material was chosen. Therefore, energy dissipation was not analyzed. At the same time, the precessional motion of the rotating C_{60} molecule could be analyzed. A similar model of the dynamic

state of fullerite nodes was used in an earlier article,[36] where the characteristic time of the reorientation of fullerenes in the fcc phase of fullerite was found. This time coincided with the measurement data was obtained using nuclear magnetic resonance.[17]

Acknowledgements

Conflict of Interest

The authors declare no conflict of interest.

Keywords

[1] H. Terrones, M. Terrones, *New J. Phys.* **2003**, *5*, 126.
[2] H. W. Kroto, J. R. Heath, S. C. O'Brien, R. F. Curl, R. E. Smalley, *Nature* **1985**, *318*, 162.
[3] S. J. Duclos, K. Brister, R. C. Haddon, A. R. Kortan, F. A. Thiel, *Nature* **1991**, *351*, 380.
[4] T. Horikawa, T. Kinoshita, K. Suito, A. Onodera, *Solid State Commun.* **2000**, *114*, 121.
[5] V. V. Ivanovskaya, A. L. Ivanovskii, *J. Superhard Mater.* **2010**, *32*, 67.
[6] S. Berber, E. Osawa, D. Tománek, *Phys. Rev. B* **2004**, *70*, 085417.
[7] S. Okada, S. Saito, A. Oshiyama, *Phys. Rev. Lett.* **1999**, *83*, 1986.
[8] J. Yang, J. S. Tse, T. Iitaka, *J. Chem. Phys.* **2007**, *127*, 134906.
[9] V. V. Brazhkin, A. G. Lyapin, *Phys.-Usp.* **1996**, *39*, 837.
[10] O. P. Chernogorova, E. I. Drozdova, I. N. Lukina, *J. Phys.: Conf. Ser.* **2020**, *1431*, 012066.
[11] V. V. Brazhkin, V. L. Solozhenko, V. I. Bugakov, S. N. Dub, O. O. Kurakevych, M. V. Kondrin, A. G. Lyapin, *J. Phys.: Condens. Matter* **2007**, *19*, 236209.
[12] V. M. Prokhorov, V. D. Blank, G. A. Dubitsky, S. Berezina, V. M. Levin, *J. Phys.: Condens. Matter* **2002**, *14*, 11305.
[13] A. Tripathi, A. Kumar, F. Singh, D. Kabiraj, D. K. Avasthi, J. C. Pivin, *Nucl. Instrum. Methods Phys. Res. B* **2005**, *236*, 186.
[14] K. L. Narayanan, N. Kojima, K. Yamaguchi, N. Ishikawa, M. Yamaguchi, *J. Mater. Sci.* **1999**, *34*, 5227.
[15] B. Todorovic-Markovic, I. Draganic, D. Vasiljevic-Radovic, N. Romcevic, M. Romcevic, M. Dramicanin, Z. Markovic, *Appl. Phys. A* **2007**, *89*, 749.
[16] F. C. Zawislak, D. L. Baptista, *Nucl. Instrum. Methods Phys. Res. B* **1999**, *149*, 336.
[17] R. D. Johnson, R. D. Johnson, C. S. Yannoni, H. C. Dorn, J. R. Salem, D. S. Bethune, *Science* **1992**, *255*, 1235.
[18] J. Shen, S. He, F. Zhuang, *Eur. Phys. J. D* **2005**, *33*, 35.
[19] S. Yangs, T. Wey, K. Scheurell, E. Kemnitz, S. I. Troyanov, *Chem. Eur* **2015**, *21*, 15138.
[20] S. V. Lubenets, L. S. Fomenko, V. D. Natsik, A. V. Rusakova, *Low Temp. Phys.* **2019**, *45*, 1.
[21] M. Raransky, V. Balazyuk, M. Gunko, A. Struk, *East.-Eur. J. Enterp. Technol.* **2015**, *5*, 18.
[22] K. Skopek, M. C. Hershberger, J. A. Gladysz, *Coord. Chem. Rev.* **2007**, *251*, 1723.
[23] C. S. Vogelsberg, M. A. Garcia-Garibay, *Chem. Soc. Rev.* **2012**, *41*, 1892.
[24] W. Setaka, K. Inoue, S. Higa, S. Yoshigai, H. Kono, K. Yamaguchi, *J. Org. Chem.* **2014**, *79*, 8288.
[25] E. Prack, C. A. O'Keefe, J. K. Moore, A. Lai, A. J. Lough, P. M. Macdonald, M. S. Conradi, R. W. Schurko, U. Fekl, *J. Am. Chem. Soc.* **2015**, *137*, 13464.
[26] S. I. Bozhko, E. A. Levchenko, V. N. Semenov, M. F. Bulatov, I. V. Shvets, *J. Exp. Theor. Phys.* **2015**, *120*, 831.
[27] P. Wolski, K. Nieszporek, T. Panczyk, *Langmuir* **2018**, *34*, 2543.
[28] J. G. Chigvinadze, S. M. Ashimov, A. V. Dolbin, *Low Temp. Phys.* **2019**, *45*, 531.
[29] M. Krause, M. Hulman, H. Kuzmany, O. Dubay, G. Kresse, K. Vietze, G. Seifert, C. Wang, H. Shinohara, *Phys. Rev. Lett.* **2004**, *93*, 137403.
[30] P. M. Rafailov, V. G. Hadjiev, A. R. Goñi, C. Thomsen, *Phys. Rev. B* **1999**, *60*, 13351.
[31] A. Piatek, A. Dawid, Z. Gburski, *J. Phys.: Condens. Matter* **2006**, *18*, 8471.
[32] V. Ya. Rudyak, *Statistical Aerohydromechanics of Homogeneous and Heterogeneous Media*, Vol. *1*, NSUACE, Novosibirsk **2005**, p. 320.
[33] L. A. Girifalco, *J. Phys. Chem.* **1992**, *96*, 858.
[34] L. A. Girifalco, *Phys. Rev. B Condens. Matter* **1995**, *52*, 9910.
[35] J. M. Ortega, *An Introduction to Numerical Methods for Differential Equations* (Ed: W. G. Poole), Pitman Publishing Ltd, Marshfield **1981**, p. 329.
[36] A. M. Bubenchikov, M. A. Bubenchikov, D. V. Mamontov, *Crystals* **2020**, *10*, 510.